RSC Advances

ROYAL SOCIETY OF CHEMISTRY

www.rsc.org/advances

Morphological and microstructural investigations of composite dielectrics for energy storage

J. Glenneberg,[a] M. Zenkner,[c] G. Wagner,[ad] S. Lemm,[c] C. Ehrhardt,[b] W. Münchgesang,[c] A. Buchsteiner,[a] M. Diestelhorst,[c] H Beige,[c] S. G. Ebbinghaus[b] and H. S. Leipner[a]

We investigated structural and dielectric properties of novel capacitors based on 0-3 composite dielectrics. For this purpose various $BaTiO_3$/$Ba(Ti,Ge)O_3$ nano scaled powders were synthesized via four different routes, namely via the sol-gel procedure, the oxalate method, the Pechini method and mixed oxide method. As the best-suited method with respect to the formation of spherical and equally sized particles without agglomeration, a sol-gel synthesized powder was chosen for further experiments. The nanoparticles were coated with E glass (CaO, MgO, Al_2O_3, B_2O_3, SiO_2), BBS glass (BaO, SiO_2, B_2O_3) or an Al_2O_3/MgO mixture. The resulting composites were annealed, sintered and afterwards covered with electrodes to fabricate ceramic composite capacitors. To identify the system best suited for energy storage applications, different matrices and $BaTiO_3$/matrix ratios were investigated. The morphology and the phase content were analyzed by electron microscopy and X-ray diffraction. An optimum grain size and distribution was obtained for a 15 wt% BBS glass mixed with a $Ba(Ti,Ge)O_3$ powder. The mixture sintered at 925 °C resulted in the best composite dielectrics not only concerning the morphology but also the dielectric data. Additionally, the BBS matrix showed no tendency to form secondary phases, while preserving a homogenous distribution of matrix element components.

1. Introduction

Energy storage is more than ever a current topic. For clean, efficient and low-cost devices, high-quality capacitors seem to be a conceivable solution, especially for short-term energy storage. In contrast to batteries, capacitors have the ability to pass hundreds of thousands charging cycles, while the charge and discharge process takes place within seconds.[1] This makes the capacitor technology not only interesting for applications regarding electromobility, but also for stationary energy storage issues. In particular the growing field of wind energy provides great potential, since upcoming wind-induced power variations can be smoothed. Barium titanate (BT) as a common material with well-known dielectric properties has already found broad applications in multilayer ceramic capacitors (MLCCs). The tetragonal ferroelectric perovskite BT has enormous potential due to its high temperature stability, its applicability for AC currents in a broad frequency range and especially its high permittivity.[2,3,4] Since pure BT exhibits a comparatively low breakdown field strength, the device efficiency is limited. To increase the energy density of the capacitor, BT particles can be embedded in a specific inorganic matrix. In this way it is possible to combine the advantages of BT with the ones of the matrix material, like high breakdown voltages and low electric conductivities. Furthermore, it is extremely difficult to achieve dense ceramics at comparatively low calcination temperatures without the application of sintering additives. Here, the glass matrix used can play an important dual role. On the one hand, it additionally may lead to an enhanced densification of the composite at lower sintering temperatures[5-12], on the other hand, the electrical properties may improve. Therefore, it is inevitable to use a suitable matrix material in the proper mixing ratio with BT, not only to avoid leakage currents or low breakdown field strengths, respectively, but also to obtain dense ceramic dielectrics at temperatures which are economic for mass production. To further decrease the sintering temperature, slight amounts of germanium can be added to the BT. Plessner et al.[13] investigated germanium-substituted BT and stated significantly lower sintering temperatures, while still obtaining dense ceramics. Since titanium and germanium differ in their ionic radii[14], the formation of the

mixed crystal is limited to a maximum germanium content of 1.8 mol% resulting in barium titanate germanate $Ba(Ti_{0.98},Ge_{0.02})O_3$ (BTG).[15-18] For cost reduction, a low calcination temperatures of the composite dielectrics is required in capacitor technology in order to use relatively cheap electrode materials like Ag/Pd. The composite dielectrics can be easily manufactured by liquid phase sintering.

Important dielectric parameters like the permittivity or the breakdown field strength, as well as the energy density of the capacitor, depend on the microstructure of the composite dielectric. As a consequence, the accurate knowledge of the microstructure as well as the morphology is mandatory in order to understand how the electrical parameters are accomplished.

To optimize the dielectric properties, it is essential to find optimum parameters with respect to the BT starting powder, the matrix material, the BT/matrix volume ratio and the fabrication route of the composite dielectrics. Specifically, the permittivity strongly depends on the BT grain size.[19,20,21] Since the grain size is closely linked to the sintering temperature, it is possible to tailor a ceramic with optimum properties by this key factor. Furthermore, the homogeneity of the matrix and the grain distribution play an important role for the efficiency of the device. The BT particles have to be completely embedded in the matrix in order to avoid leakage currents and low breakdown voltages or ohmic resistances, respectively. To attain the maximum permittivity of the BT particles, grain sizes of about 1 µm are intended. This goal can only be achieved with the proper matrix and BT/matrix ratio, since the matrix can act as a grain growth inhibitor during sintering. Furthermore, a homogenous distribution of the BT particles within the respective matrices is desired to prevent the occurrence of leakage current paths, which would lead to a rapid discharge of the prepared capacitor. For this purpose, we want to implement two different promising and easy methods. The precipitation and the spray drying method provide the best prerequisites to achieve a homogenous distribution of the BT particles within the matrix, since the glass formation takes place during the final heat treatment. This is a very important advantage over the common mortar and pestle or ball milling methods, because the degree of mixing the components is on a better level.

In this paper, we report on a materials strategy for the fabrication of capacitors as energy storage devices. Different methods for the synthesis of BT starting powders and the application of different matrix materials will be discussed, while concentrating on the investigation of the relation between the microstructure and the properties of the composite dielectrics. We mainly focus on the effect of different synthesis processes and materials on the morphology and existing phases. The discussion of important dielectric parameters will be limited in this paper to the influence of the different matrices and BT/matrix ratios on the permittivity of the dielectrics fabricated. Further details on the characterization of the dielectric properties will be published elsewhere.

2. Experimental

2.1 Materials

$BaTiO_3$/$Ba(Ti/Ge)O_3$ nanoparticles were synthesized via three different soft chemical methods, namely the sol-gel method, the oxalate method, and the Pechini method. Additionally, BT/BTG starting powders were prepared by the conventional mixed-oxide method. On the one hand, the three soft chemical methods have been chosen because it is well known, that soft chemical methods provide highly pure products, since the chemical reactions can take place at the atomic scale. On the other hand, the mixed-oxide method was additionally investigated as a much higher amount of material can be synthesized, which may be important for a later application-orientated process. To prevent agglomeration, the synthesized nanoparticles were embedded in a special glass matrix. In the following, the four synthesis methods and the matrix preparation are described.

2.1.1 Sol-gel synthesis. Starting from titanium (IV) chloride (60 mmol, >99 %, Acros) or a mixture of titanium (IV) chloride (58.8 mmol) and germanium (IV) chloride (1.2 mmol, >99 %, Merck) dissolved at 0 °C in ethanol, an equimolar aqueous solution of barium chloride ($BaCl_2$) (667 mmol/l, >98 %, Merck) was added slowly. Afterwards an excess aqueous KOH solution was added to achieve precipitation:

$$BaCl_2 + TiCl_4 + KOH \rightarrow BaTiO_3 + 3H_2O + 6KCl \quad (1)$$

$$BaCl_2 + (1\text{-}x)TiCl_4 + xGeCl_4 + 6KOH \rightarrow Ba(Ti_{1-x})/Ge_x)O_3 + 3H_2O + 6KCl,\ x=0.02 \quad (2)$$

The obtained gel was heated under reflux in argon atmosphere for 6 h. After cooling, the residue was filtered off, washed three times with 50 ml distilled water and then two times with 50 ml ethanol as well as with acetone. Finally, the reaction product was dried in air.[22]

2.1.2 Oxalate method. Titanium (IV) i-propoxide (30 mmol, >99 %, Merck) was added dropwise to an aqueous solution of oxalic acid (90 mmol). The reaction mixture was stirred at 80 °C until a clear solution was obtained. Afterwards barium acetate (30 mmol, >98 %, Merck) was added and the resulting suspension was further heated for 1 h.

$$Ba(CH_3OO)_2 + Ti(OC_3H_7)_4 + 2H_2C_2O_4 + 5H_2O \rightarrow BaTiO(C_2O_4)_2{\cdot}4H_2O + 4C_3H_7OH + 2CH_3COOH \quad (3)$$

$$BaTiO(C_2O_4)_2{\cdot}4H_2O + O_2 \rightarrow BaTiO_3 + 4CO_2 + 4H_2O \quad (4)$$

The solid powder obtained was separated by filtration, washed three times with 50 ml distilled water, two times with 50 ml ethanol and subsequently dried in air.[23]

2.1.3 Pechini method. Titanium (IV) i-propoxide (30 mmol, >99 %, Merck) was slowly added to a mixture of an aqueous solution of citric acid (120 mmol) and excess 1,2-ethanediol. The mixture was then heated to 80 °C and barium acetate (30 mmol, >98 %, Merck) was added. After raising the reaction temperature to 120 °C a yellow gel was obtained that finally decomposed to a brownish resin.

$$Ba(CH_3COO)_2 + Ti(OC_3H7)_4 + 3C_6H_8O_7 \rightarrow BaTi(C_6H_6O_7)_3 + 4C_3H_7OH + 2CH_3COOH \quad (5)$$

$$BaTi(C_6H_6O_7)_3 + 2C_2H_6O_2 \rightarrow \text{gel/resin} \rightarrow BaTiO_3 \quad (6)$$

The brown resin was annealed at 400 °C in a muffle furnace for 2 h and the resulting black powder was grinded intensively. The final reaction to a white BT powder was achieved by annealing for eight hours at 640 °C.[24]

2.1.4 Mixed oxide method. Barium carbonate (>99 %, Solvay), titanium (IV) oxide (>99 %, Merck) and germanium (IV) oxide (>99 %, Riedel-de Häen) were separately milled with distilled water and agate balls in PVC grinding drum for 24 h. Afterwards, the slurry was filtered and then annealed at 500 °C for 2 h. The obtained cleaned and dried powders of $BaCO_3$ and TiO_2 (and GeO_2) were mixed together in the respective stoichiometric ratio and grinded together with propan-2-ol and agate grind balls for another 24 h. The resulting mixture was filtered off and dried at 120 °C for 24 h followed by an annealing step at 1200 °C for 2 h.[16]

$$BaCO_3 + TiO_2 \rightarrow BaTiO_3 + CO_2 \quad (7)$$

$$BaCO_3 + (1\text{-}x)TiO_2 + xGeO_2 \rightarrow Ba(Ti_{1-x}/Ge_x)O_3 + CO_2,\ x=0.02 \quad (8)$$

2.1.5 Coating. To avoid agglomeration of the individual BT/BTG particles three different glass materials were used. In the following, the compositions and ratios of these matrices are listed (a-c).

a) Al_2O_3/ MgO: 50.0 wt% Al_2O_3 [$Al(NO_3)_3{\bullet}9H_2O$], 50.0 wt% MgO [$Mg(NO_3)_2{\bullet}6H_2O$],
b) E glass: 17.5 wt% CaO [$Ca(NO_3)_2{\bullet}4H_2O$], 4.5 wt% MgO [$Mg(NO_3)_2{\bullet}6H_2O$],
14 wt% Al_2O_3 [$Al(NO_3)_3{\bullet}9H_2O$], 10 wt% B_2O_3 [H_3BO_3],
54 wt% SiO_2 [TEOS],
c) BBS glass: 30 wt% BaO [$Ba(ac)_2$], 60 wt% B_2O_3 [H_3BO_3], 10 wt% SiO_2 [TEOS].

As starting materials for the final glass matrices, soluble chemicals like nitrates, acetates or acids of the respective cations were used. The coatings were then applied to the BT/BTG starting powders by precipitation or spray drying as described more detailed in the next section.

2.2 Preparation of the composite capacitor samples

The different fabrication steps of the ceramic composite capacitors are summarized in Fig.1.

The composite suspension was prepared by mixing the BT/BTG powders with the glass component starting agents, which were dissolved in propane-2-ol. To prevent aggregation of the nanoparticles, the mixture was dispersed in an ultrasonic bath for 6 h. Afterwards, two different ways of particle coating were applied, namely spray drying and precipitation. These two coating methods led to different results and are discussed below. Both the spray drying and the precipitation method were used to achieve uniform distributions of the coated particles. Concerning the precipitation method, the composite suspension was heated up to 70 °C, while stirring the mixture. The glass components precipitated caused by a dropwise addition of a 10 % ammonia solution. After further heating of the solution, the solid constituents were centrifuged and finally dried at 120 °C in air for 2 h. For the spray drying method the Büchi mini spray dryer B-191 was used. The air flow and temperature were set to 600 l/min and 140 °C. While bigger agglomerates remained in the spray cylinder, the coated nanoparticles were collected in a cyclone. Similar to the precipitate method, the formation of the glass matrix took place during a final heat treatment. By application of both coating methods, BT/BTG particles embedded in glass matrix could be obtained. These particles were pressed into dense compacts.

Afterwards these green compacts were annealed at 500 °C for 1 h and finally sintered at different temperatures ranging from 900 to 1400 °C for 1 h. Through solid-state reaction, a grain growth occurred in the composite dielectric, and the material was additionally densified. Finally, sintered compacts with a diameter of about 5 mm and a thickness of 0.5 to 1 mm corresponding to the amount of material used were achieved. To obtain parallel plate capacitors for electrical measurements, the composite dielectrics were contacted with thin films of conductive silver on the top and bottom sides of the compact.

2.3 Measurements

Scanning electron microscopy (SEM) was carried out with a Philips ESEM XL 30 FEG environmental scanning electron microscope. For transmission electron microscopy (TEM), a Philips CM 200 with an additional scanning transmission electron microscope unit (STEM) was used. Both microscopes offered the opportunity to perform electron dispersive X-Ray spectroscopy (EDS) to reveal chemical information. At the SEM, qualitative energy-dispersive X-ray spectroscopy was possible, while at the TEM both qualitative and quantitative EDS measurements were feasible. The chemical phase purity of the starting powders as well as their particles sizes and the crystalline phases of the composite dielectrics were determined by X-ray diffraction using a Bruker D8 diffractometer with CuKα radiation in the angular range of $2\theta = 20 - 80°$ with a step size of 0.01° (2θ) To investigate particle sizes of the pure and coated starting powders, gas physisorption was done using a Nova 1000 surface area analyzer (Quantachrome Corporation) the Brunauer–Emmett–Teller (BET) model was applied for data evaluation.

Non-isothermal dilatometry was used to determine the thermal expansion/shrinkage and the density with a Setaram TMA 92 thermomechanical analyzer. A Hewlett Packard 4284A precision LCR meter was used for frequency-dependent capacitance measurements. The investigations were carried out at room temperature at a constant voltage of 1 V in the frequency range of 120 to $1 \cdot 10^6$ Hz.

3. Results and Discussion

3.1 Starting powders

The BT/BTG starting powders differed strongly in their grain sizes, morphologies, and particle distributions depending on the synthesis routes as shown in Figure 2. The particles prepared by the oxalate and the pechini method (Fig. 2b and c) tended to build up huge agglomerates. The agglomerates formed by the oxalate method had a rhombical shape and consisted of individual particles with a size of about 60 nm as determined by SEM. In case of the Pechini method, large flakes could be observed (Fig 2c), while the size of the individual particles could not be determined by SEM. As a consequence of the tendency to form firm agglomerates, starting powders from these two synthesis methods were not used for further experiments. In contrast, BT synthesized by the sol-gel method showed nearly no agglomeration as seen in Fig. 2a. Spherical particles with an average particle size of 50 nm were obtained with a small range of particle size distribution. The particles formed by the mixed-oxide method did not show the high degree of agglomeration of the oxalate or Pechini methods, but due to the high calcination temperature of 1200 °C the typical particle size was about one magnitude larger (in the range of 200 to 1000 nm) compared to the sol-gel synthesis. To verify the particle sizes determined by electron microscopy, gas physisorption and X-ray powder diffraction were applied. These methods confirmed the results of electron microscopy as listed in Tab. 1.
While the sol-gel and the mixed oxide method provided the best results with regard to the particle distribution, the particle size from the sol-gel synthesis with an average of 40 nm were best suited for our purposes. Due to the high calcination temperature of 1100 °C, the grain growth of the mixed-oxide powder resulted in much bigger particles than, obtained with the soft chemical methods In summary, the starting powder from the sol-gel procedure was the most promising and all further studies were carried out with this material.

3.2. Composite dielectrics

To investigate the influence of the matrix on morphological and electrical properties of the composite dielectrics, a series of different weight ratios of the matrix to the sol-gel starting powder was tested. The aim was to obtain a uniform distribution of particles within the matrix.

3.2.1 Composites with Al_2O_3/MGO matrix. First attempts to fabricate composite dielectrics with an Al_2O_3/MgO matrix (see Fig. 3) showed that such a matrix was not well suited. XRD experiments revealed a considerably high amount of crystalline $BaAl_2O_4$ in addition to BT. This extra phase formed large needle-shaped grains as shown in Figure 3. Since a corundum phase did not form, a side reaction of the BT starting powder with alumina is assumed during the sinter process.
With the observed high amounts of the $BaAl_2O_4$ spinel phase, a separation of the BT nanoparticles was not possible. In turn, high leakage currents, which led to a fast discharge of the capacitors, were observed in the electrical measurements.

3.2.2 Composites with E glass matrix. The compacts containing the E glass were already analyzed after the first annealing step of 500 °C. These compacts exhibited big amorphous flakes of the matrix phase with partial agglomerations of BT particles as shown in Fig. 4. Macroscopically, this was related to a rather low density and rather brittle compacts. The annealing temperature of 500 °C was appropriate to decompose residual nitrates or carbonates. Additionally, we were able to verify that at temperatures below 500 °C no grain growth of BT took place, since the nanoparticles still had sizes of about 50 to 60 nm.
TEM/EDS studies of E glass-coated green compacts revealed a homogenous matrix composition, as well as the expected ratios of matrix components. Three different positions (Fig. 4, positions 1, 2, 3) were analyzed by EDS point measurements. These revealed a uniform composition of the different matrix flakes with an average amount of 7.2 at% Si, 2.2 at% Al and 3 at% Ca. It should be noted that the additionally found Ba and Ti correspond to the

contribution of the surrounding BT particles. The amount of the magnesium constituent was only 0.1 at% and therefore below the detection limit. Consequently, no Mg signal was detected.

Exemplarily for a ceramic with E glass coated BT, Fig. 5 shows a sample with 15 wt% E glass sintered at 1100 °C. The presented SEM image taken with back-scattered electrons (BSE) shows a uniform grain size distribution with particle sizes of 0.8 to 1 µm. According to Arlt et al. [18], this corresponds approximately to the optimum grain size for the highest permittivity. In addition, the particles were homogenously distributed within the matrix. On the other hand, EDS investigations revealed the presence of additional phases besides the E glass component. These undesired crystalline phases can be recognized by their darker contrast in the BSE image (Fig. 5). The material was identified as a mixture of fresnoite ($Ba_2TiSi_2O_8$) and barium aluminium silicate ($BaAl_2Si_2O_8$) by XRD measurements (Fig. 6).

The presence of the secondary phases indicates a reaction of the BT particles with the matrix components. Samples with only 3 wt% of E glass did not show any sign of fresnoite. However, in this case, the small amount of the matrix cannot fully coat the BT particles. As a consequence of the secondary phases and/or the incomplete BT coating, high leakage currents were measured in the compacts with E glass, regardless of the amount of the matrix constituent. To avoid a reaction between E glass and the BT powder, the sintering temperature was lowered to 1000 °C, but density studies by nonisothermal dilatometry showed that only porous samples could be obtained at this lower temperature.

As shown in Fig. 7, the matrix exhibited a rather inhomogeneous element distribution. Since the silicon signal was detected at every position where no barium was present, silicon is the only element, which is spread over the entire matrix. In contrast, aluminium, magnesium and especially calcium are only partially to find. Although the E glass matrix exhibited a highly homogenous composition after the first annealing step, as shown in Fig. 4, a separation of the matrix elements can be concluded during the final sintering. In conclusion, the E glass matrix turned out to be not well suited due to its tendency to form extra phases, which prevent a complete coating of BT. It is supposed that a matrix consisting of five different elements can hardly be controlled since a segregation of some constituents is probable. Concerning the influence of the E glass coating matrix on electrical data, another disadvantage occurred, as the permittivity decreases upon coating with E glass. While the permittivity of pure BT was quite high (Fig. 8), it drastically decreased with increasing amount of E glass. Since a higher amount of the matrix material is required to achieve a low leakage current, it is inevitable to lose permittivity, which leads to an enormous reduction of efficiency. E glass is therefore not applicable as a matrix for BT particles in high efficient dielectrics.

3.2.3 Composites with BBS glass matrix. BBS glass turned out to be the most promising candidate for composite dielectrics. The BBS glass consists of only three elements, and no inhomogeneous distribution of the single constituents was found. A uniform formation of the BBS glass matrix always occurred independent of the amount of the matrix material and the sintering temperatures applied.

Just as in the case of the E glass, the BBS green compacts showed no sign of grain growth at 500 °C. Conversely, calculations based on the XRD experiments and SEM images showed that the grains coated with BBS glass exhibit a reduced grain growth at comparable calcinations temperatures and matrix ratios. We assume that BaO inhibits the material transport and therefore the fine grain structure is preserved with respect to the sintering temperature.

The coating of BT by BBS glass for the samples shown in Fig. 9 was done via the precipitation method. SEM images of the compacts after sintering (Fig. 9 left) showed on the surface needle-or plate-shaped BT crystals with strongly varying sizes in addition to the globular grains intended. The SEM image of the grain structure, after polishing, revealed only spherical particles. The majority of these BT particles were completely surrounded by the matrix, which resulted in a much lower leakage current as discussed below.

In contrast to the samples prepared by the precipitation method, only globular particles were found using the spray drying method. Furthermore, a nearly perfect covering of the individual BT particles with the matrix was achieved. A coating with a 10 wt% matrix leads to a bimodal grain growth, where grains with a size of about 8 µm and smaller particles with a size of about 2 µm were formed (Fig. 10a). Further studies of the grain structure of a spray

dried ceramic with a 15 wt% BBS matrix after the same sintering temperature revealed after polishing a very uniform grain size distribution. The grain size determined by SEM was about 4 µm as shown in Fig. 11b. From the very similar brightness of the BSE SEM images a high chemical homogeneity is expected. To verify this anticipated chemical uniformity, EDS experiments were carried out. Only two different kinds of spectra were found, namely that of crystalline BT and that of the amorphous BBS glass matrix.

Best results were achieved using germanium as an additional sintering additive. Fig. 11 shows a sol-gel BTG ceramic with 15 wt% BBS glass sintered at 1050 °C. Uniform grains with an average grain size of 6 µm were formed. A nearly perfect coating of the individual BT particles was achieved. The chemical purity of the phases was proved by SEM EDS. Due to the better stability of BT compared to BTG at higher temperatures germanium should diffuse from the BTG towards the surrounding glass matrix.

As confirmed experimentally, prior to sintering the matrix was Ge-free and the BT contains about 0.2 % Ge. After sintering at 950 °C the BT grains are totally Ge-free, however, now the glass contains the weighed out Ge. Thus no residual germanium was found within the BT.

Consequently this process of germanium segregation didn't take place due to a concentration gradient, but is to explain by the means of the different stabilities of BT respectively BTG at higher temperatures. A clear advantage of the application of germanium is the observed decrease in the sintering temperature. Even at 925 °C dense compacts (ρ = 93 %) were obtained.

To determine the amount of germanium within the matrix and to investigate the uniformity of its distribution, TEM EDS point measurements were done. EDS point measurements were carried out in the BT particles and in the BBS matrix (Fig. 12). A constant ratio corresponding to the BT stoichiometry expected was obtained with a narrow fluctuation of about 1 at%, which is related to the typical error of EDS measurements. Within the BT particles no germanium signal could be found, which indicates a complete diffusion of germanium from the BT particles into the matrix. The uniformity of the distribution of germanium within the matrix was investigated. Except for position 9 (Fig. 12), a constant composition and a homogenous distribution of the matrix was obtained. Disregarding the data measured at position 9, an average composition of 3.5 at% SiO_2, 17.4 at% GeO_2 and 79.1 at% BaO was determined, which matches roughly the expected elemental components. The B_2O_3 component could not be defined, because its characteristic X-ray radiation is absorbed by the used beryllium window of the EDS system. 950 °C turned out to be the best sintering temperature for this material system, as it provided an optimum grain size. According to literature data, the ideal grain size for the highest dielectric constant lies between 0.7 and 2 µm[18,19,20], whereas higher sintering temperature leads to the formation of larger BT particles and lower permittivities.

The permittivity was only slightly affected by the amount of the BBS matrix. Electrical measurements indicated a small decrease in the permittivity with increasing matrix content, but the effect was much less pronounced than for the E glass. The low dependence of the permittivity on the matrix amount in addition with the found low leakage currents are an evidence for nearly isolated BT particles.

With the BBS glass coating, composite dielectrics with high efficiencies could be fabricated. The material was free of impurity phases and only low sintering temperatures had to be used. Furthermore, the BT particles had an optimum grain size, a high degree of uniformity and the required electrical isolation was obtained. Thus, composite dielectrics made of BTG particles with a BBS glass matrix are promising materials for applications in the field of energy storage.

4. Conclusions

We were able to synthesize phasefree BT particles via four different procedures, namely the sol-gel method, the oxalate method, the Pechini method as well as the mixed-oxide method.

According to our investigations, the sol-gel route gave the best results as spherical particles with a narrow grain size distribution and a low degree of agglomeration were obtained. In contrast, the mixed-oxide method resulted in a broad size distribution, preventing a further application of such BT powders. Starting material formed by the oxalate and the Pechini method are not suitable for embedding in a glassy matrix because of the formation of firm agglomerates.

Three different matrix materials were investigated, namely the Al_2O_3/MgO matrix, E glass consisting of SiO_2, CaO, Al_2O_3, B_2O_3 and MgO as well as BBS glass, containing BaO, SiO_2 and B_2O_3. The coating material was applied to the BT nano particles by spray drying or precipitation method. Composite dielectrics using the Al_2O_3/MgO matrix showed the formation of the $BaAl_2O_4$ spinel, while the anticipated corundum coating could not be detected. Also the E glass coating was not suitable for further application. Although E glass ceramics showed optimum BT particle sizes and homogenous particle distributions, the occurrence of additional phases, like the fresnoite phase shown, was inevitable when higher amounts of the matrix were used. Furthermore, inhomogeneities after sintering and the strong dependence of the permittivity on the amount of the matrix made the E glass matrix unsuitable for capacitor applications. Best results were obtained with 15 wt% BBS glass as a coating of BTG starting powders synthesized by the sol-gel procedure. The most effective coating was achieved by the spray drying method. As a result, dense composite dielectrics at comparatively low sintering temperatures could be fabricated. The particle size and distribution together with the separation by the coating matrix was found to be best among the material systems tested. The BBS matrix showed no tendency to form extra phases independent of the sintering temperatures and the matrix ratios used. Regardless of the amount of the matrix coating, high permittivities were realized.

Acknowledgements

This work was funded by the German Bundesministerium für Bildung und Forschung (BMBF) within the ForMaT/SuperKon initiative.

References

[a] Interdisziplinäres Zentrum für Materialwissenschaften, Martin-Luther-Universität Halle-Wittenberg, Heinrich-Damerow-Straße 4, 06120 Halle (Saale), Deutschland

[b] Institut für Chemie, Martin-Luther-Universität Halle-Wittenberg, Kurt-Mothes-Straße 2, 06120 Halle (Saale), Deutschland

[c] Institut für Physik, Martin-Luther-Universität Halle-Wittenberg, Von-Danckelmann-Platz 3, 06120 Halle (Saale), Deutschland

[d] Institut für Mineralogie, Kristallographie und Materialwissenschaft, Universität Leipzig, Scharnhorststraße 20, 04275, Deutschland

1 P. Ball, *MRS Bull.*, 2012, **37**, 802-803.

2 C. Pithan, D. Hennings and R. Waser, *Int. J. Appl. Ceram. Technol.*, 2005, **1**, 1.

3 A.J. Moulson and J.M. Herbert, in *Electroceramics: Materials, properties, applications*, ed. A.J. Moulson and J.M. Herbert, John Wiley & Sons Ltd., West Susse, 2nd edn., 2003, ch. 4, pp 159-172.

4 P.P. Phule and S.H. Risbud, *J. Mater. Sci.*, 1990, **25**, 1169.

5 K.R. Chowdary and E.C. Subbarao, *Ferroelectrics*, 1981, **37**, 689.

6 I. Burn, *J. Mater. Sci.*, 1982, **17**, 1398.

7 J.M. Haussonne, G. Desgardin, P.H. Bajolet and B. Raveau, *J. Am. Ceram. Soc.*, 1983, **66**, 801.

8 G. Desgardin, I. Mey and B. Raveau, *Am. Ceram. Soc.*, Bull. 1985, **64**, 563.

9 A.N. Virkar and S.K. Sundaram, *Trans. Indian Ceram. Soc.*, 1985, **44**, 71.

10 S.K. Sarkar and M.L. Sharma, *Mater. Res. Bull.*, 1989, **24**, 773.

11 S.F. Wang, T.C.K. Yang, W. Huebner and J.P. Chu, *J. Mater. Res.*, 2000, **15**, 407.

12 C.F. Yang, L. Wu and T.S. Wu, *J. Mater. Sci. Lett.*, 1992, **11**, 1246.
13 K.W. Plessner and R. West, *Proc. Phys. Soc. B*, 1955, **68**, 1150.
14 R.D. Shannon, *Acta Cryst. A*, 1976, **32**, 751.
15 J.P. Guha and D. Kolar, *J. Mater. Sci.*, 1972, **7**, 1192.
16 M. Zenkner, diploma thesis, Martin-Luther-Universität Halle-Wittenberg, 2006.
17 P. Baxter, N.J. Hellicar and B. Lewis, *J. Am. Ceram. Soc.*, 1959, **42**, 465.
18 R. Köferstein, L. Jäger, M. Zenkner and S.G. Ebbinghaus, *Mater. Chem. Phys.*, 2010, **119**, 118.
19 G. Arlt, D. Hennings and G. de With, *J. Appl. Phys.*, 1985, **58**, 1619.
20 T.M. Shaw, S. Trolier-McKinstry and P.C. McIntyre, *Ann. Rev. Mater. Sci.*, 2000, **30**, 263.
21 W.R. Buessem, L.E. Cross and A.K. Goswami, *J. Am. Ceram. Soc.*, 1966, **49**, 36.
22 X. Wang, B.I. Lee, M.Z. Hu, E.A. Payzant and D.A. Blom, *J. Mater. Sci.: Mater. Electron.*, 2003, **14**, 495.
23 M. Stockenhuber, H. Mayer and J. A. Lercher, *J. Am. Ceram. Soc.*, 1993, **76**, 1185-90.
24 Z. Ž. Lazarević, M. Vijatović, Z. Dohčević-Mitrović, N. Ž. Romčević, M.J. Romčević, N. Paunović and B.D. Stojanović, *J. Eur. Ceram. Soc.*, 2010, **30**, 623-628.

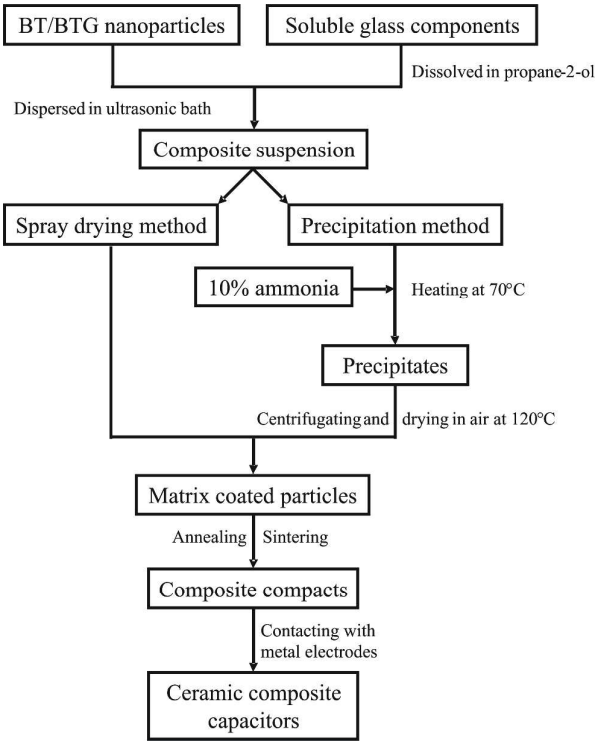

397

398 **Figure 1.** Scheme of the preparation of a ceramic composite capacitor

399

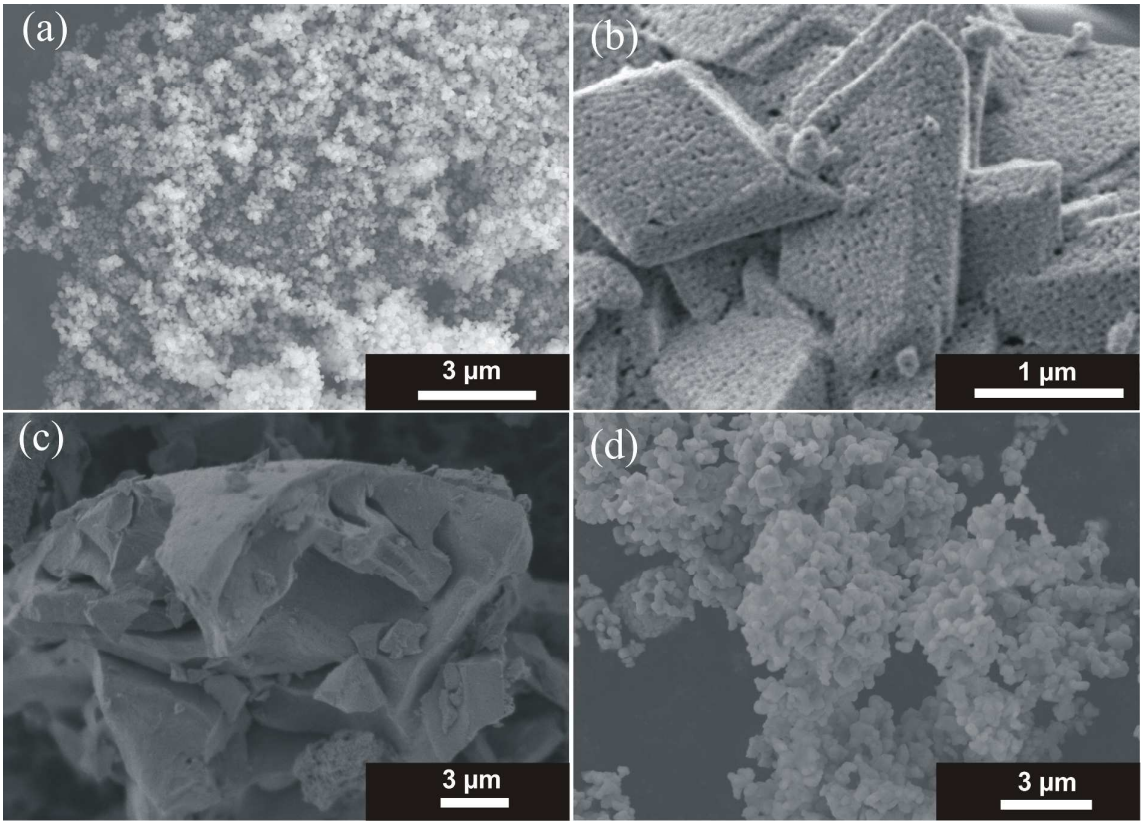

Figure 2. SEM images of $BaTiO_3$ particles synthesized by the (a) sol-gel procedure, (b) oxalate method, (c) Pechini method and (d) conventional mixed oxide method

405 Table 1. Particle sizes determined from electron microscopy images (SEM/TEM), gas physisorption (BET) and powder X-ray
406 diffraction (Scherrer equation)

407

Method	SEM/TEM d [nm]	BET d [nm]	XRD d [nm]
Sol-gel	≈ 50	25 – 35	≈ 30
Pechini	–	≈ 65	≈ 35
Oxalate	≈ 60	≈ 85	≈ 30
Mixed oxide	200 – 1000	200 – 900	–

408

409

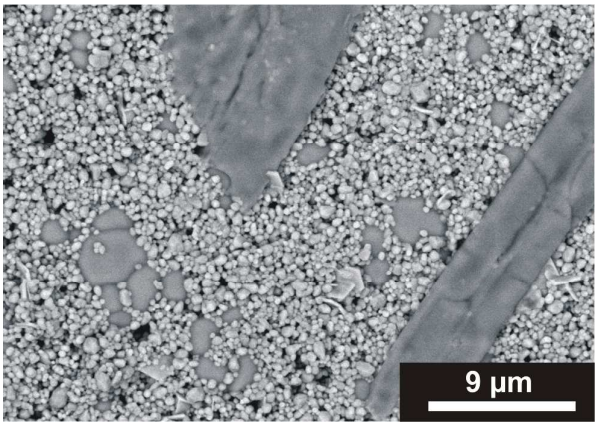

Figure 3. SEM BSE (back-scattered electrons) image of a sol-gel ceramic with an Al_2O_3/MgO matrix coating sintered at 1270 °C

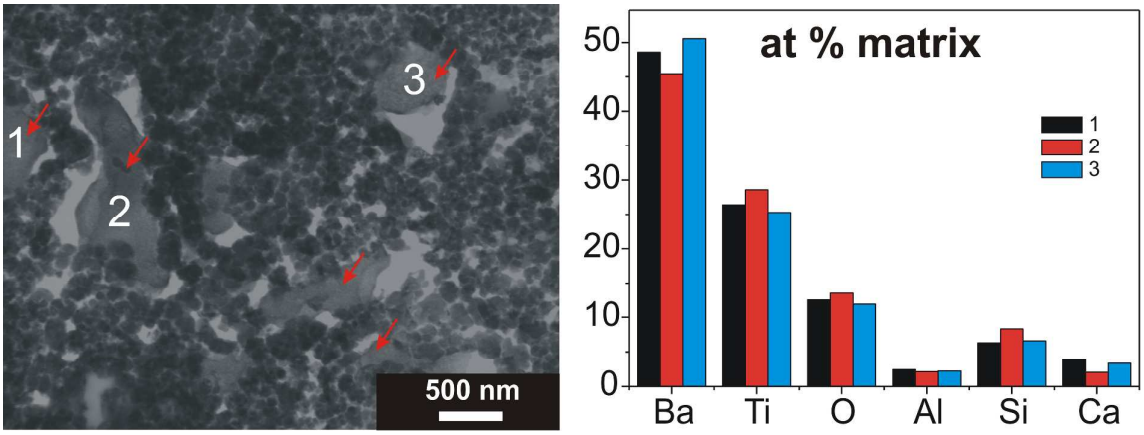

Figure 4. TEM bright-field image of a 3 wt% E glass coated sol-gel BT green compact. The matrix is marked by red arrows in the left picture. The compositions of EDS point measurements at positions 1–3 are given on the right

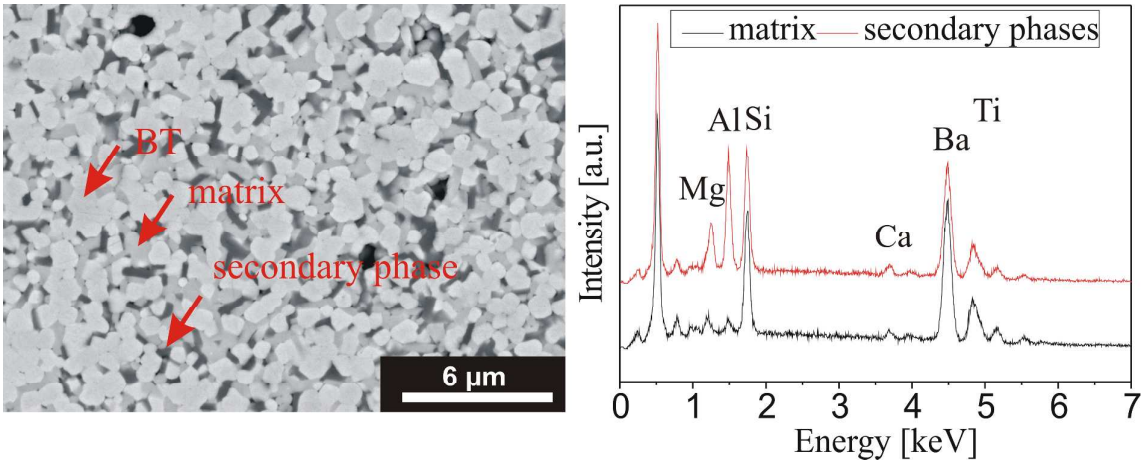

417

418 Figure 5. SEM BSE image of sol-gel BT coated with 15 wt% E glass and corresponding EDS spectra of the E glass (black) and the fresnoite
419 and barium aluminium silicate secondary phases (red)

420

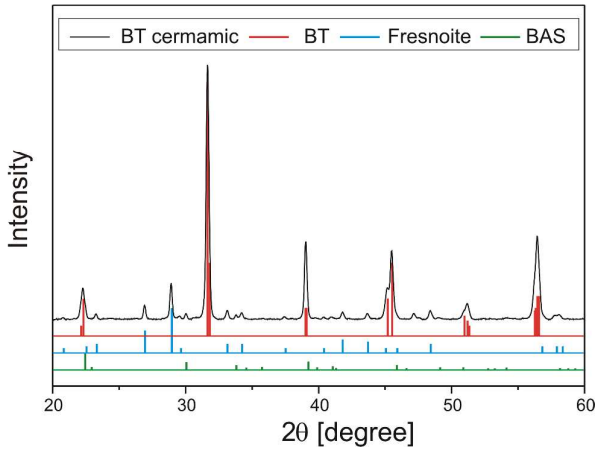

Figure 6. XRD pattern of a sol-gel BT ceramic coated with 15 wt% E glass (black). The contributing lines of BT, the fresnoite and barium aluminium silicate (BAS) phase are shown by red, blue and green markers, respectively.

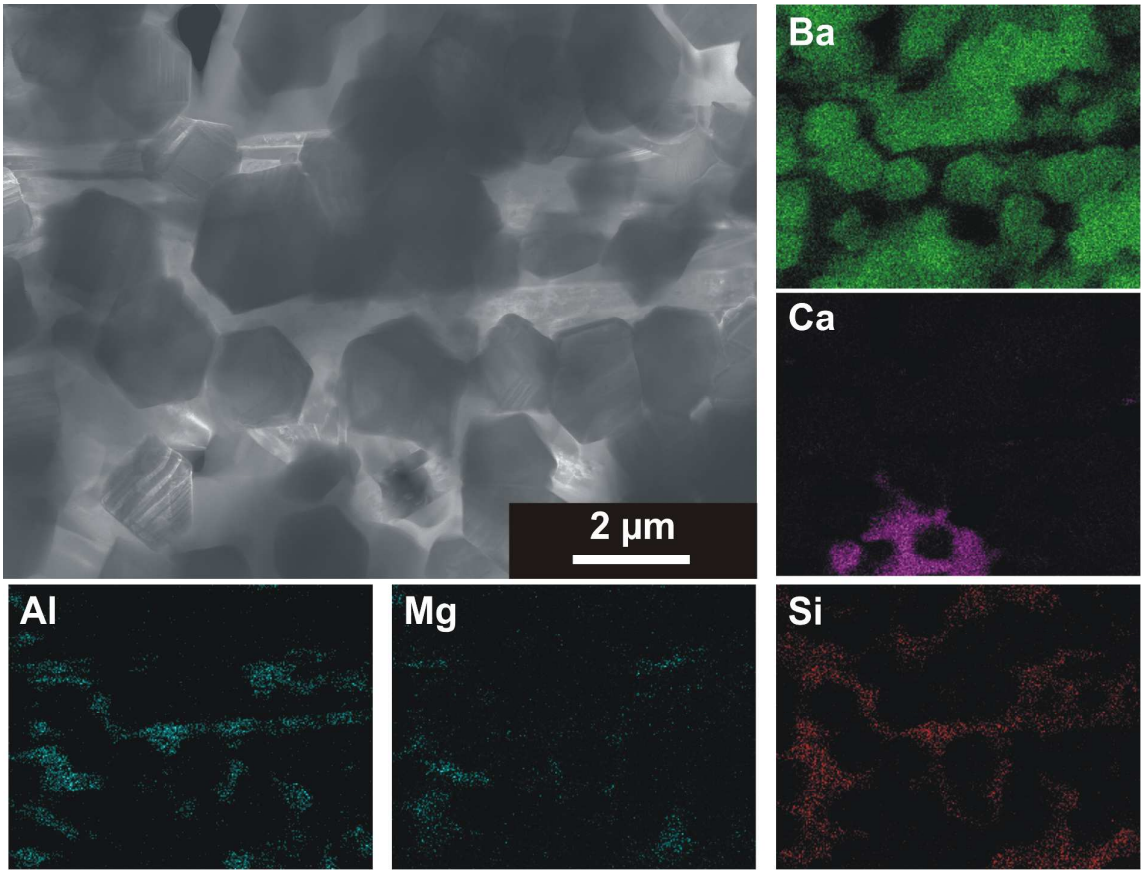

Figure 7. STEM dark-field image of sol-gel BT particles embedded in E glass matrix with corresponding EDS element mappings

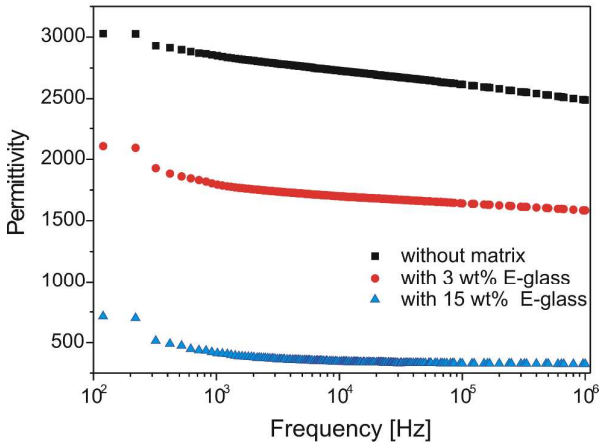

Figure 8. Permittivity of sol-gel BT ceramics as a function of the frequency and the amount of E glass

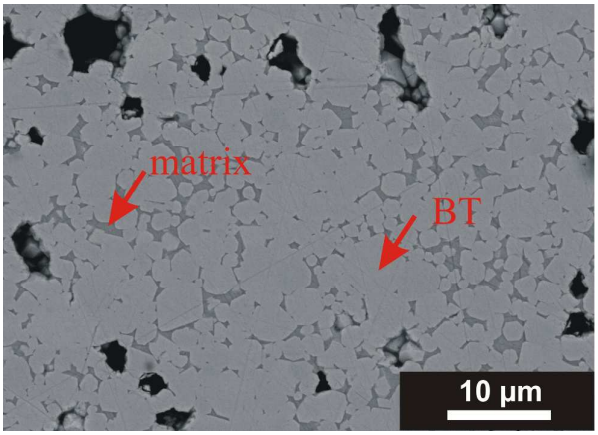

Figure 9. SEM BSE image of the grain structure after polishing of a sol-gel BT ceramic sintered at 1000 °C with 3 wt% BBS glass coated via the precipitation method

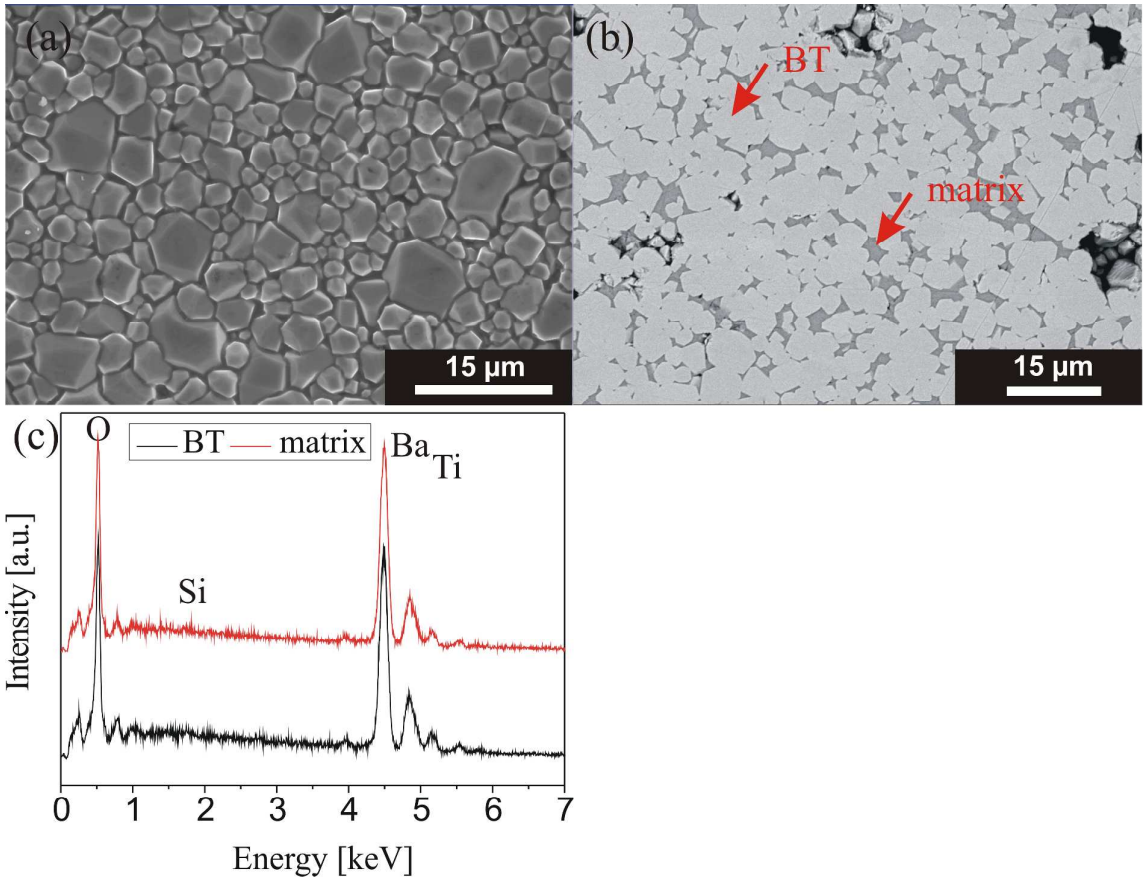

Figure 10. BSE image of (a) the surface of a sol-gel BT ceramic with 10 wt% BBS glass coated by the spray drying method, (b) the grain structure after polishing of a sol-gel BT ceramic with 15 wt% BBS glass coated by the spray drying method. The corresponding EDS spectra of BT and the BBS matrix are given in (c). The ceramics were sintered at 1000 °C.

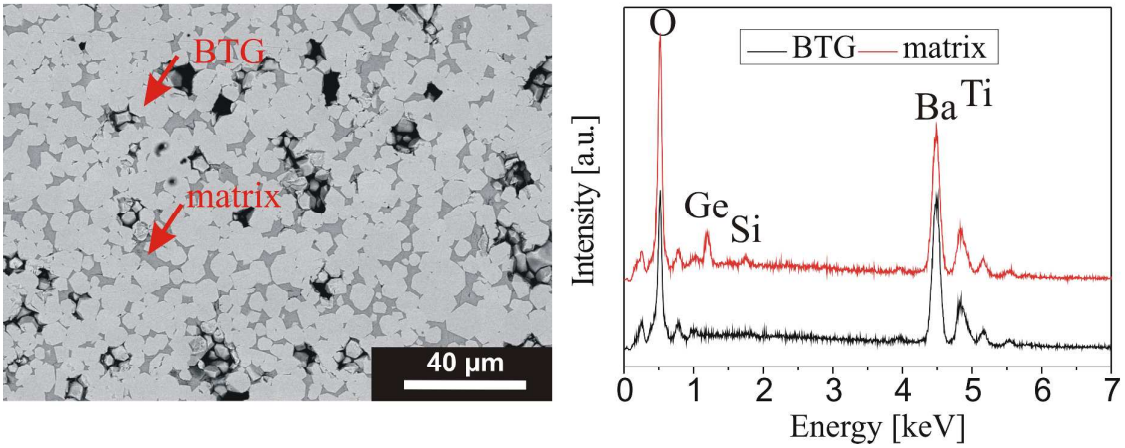

Figure 11. BSE image (*left*) of the grain structure after polishing of a sol-gel BTG ceramic with 15 wt% BBS glass coated by the spray drying method and sintered at 1050 °C. The corresponding EDS spectra of BTG and the BBS glass matrix with germanium are shown on the right.

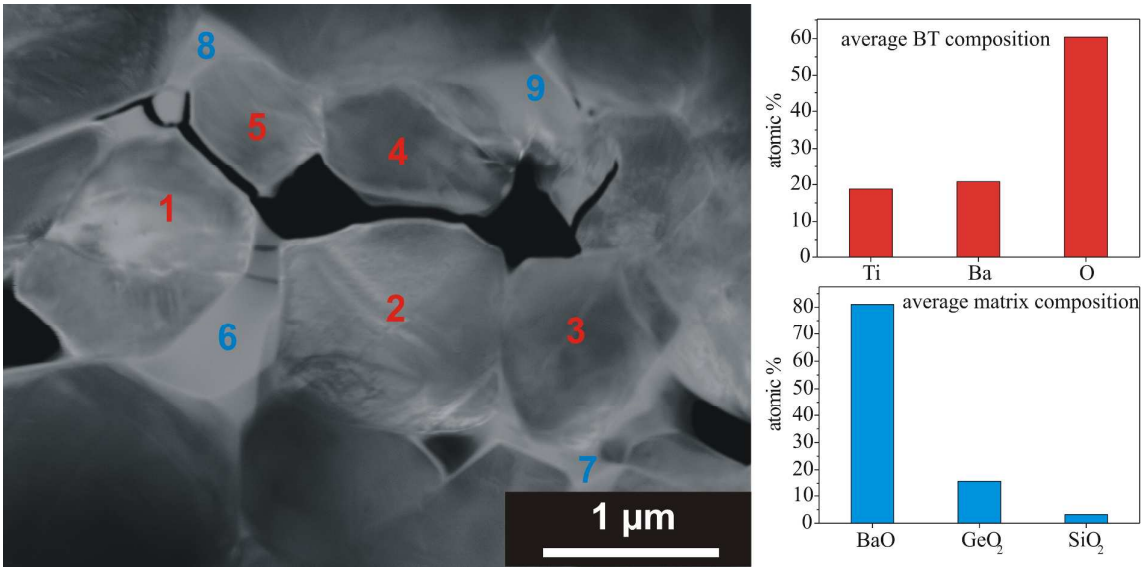

Figure 12. STEM dark-field image of a sol-gel BTG ceramic with 3 wt% BBS glass coated by the spray drying method and sintered at 950 °C. The composition determined by EDS at the positions 1–9 (1–5 BT, 6–9 matrix) is given on the right

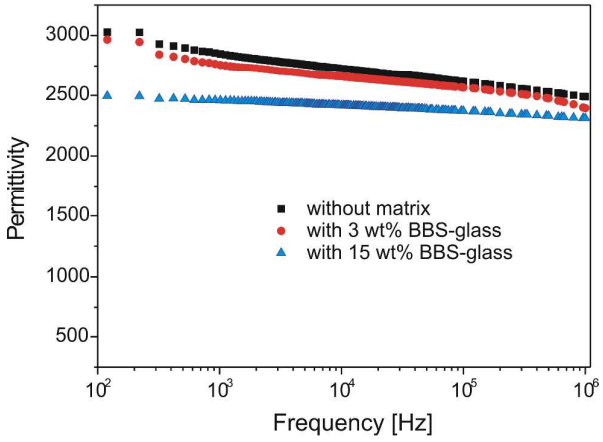

Figure 13. Permittivity of sol-gel BT ceramics as a function of the frequency and the amount of BBS glass

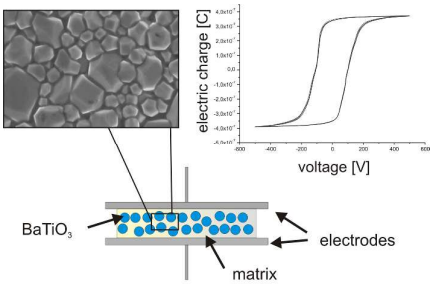

TOC: Efficient composite dielectrics can be created by combination of phase free $Ba(Ti_{(1-x)}Ge_x)O_3$ nano particles, and an inorganic BBS glass matrix, consisting of BaO, B_2O_3 and SiO_2.